A probability-box-based method for propagation of multiple types of epistemic uncertainties and its application on composite structural-acoustic system

Wenqing Zhu[1], Ning Chen[1, *], Jian Liu[1], Michael Beer[2,3,4]

[1]State Key Laboratory of Advanced Design and Manufacturing for Vehicle Body, Hunan University, Changsha 410082, China

[2]Institute for Risk and Reliability, Leibniz Universität Hannover, Callinstr. 34, Hannover, Germany

[3]Institute for Risk and Uncertainty, University of Liverpool, Peach Street, L69 7ZF Liverpool, United Kingdom

[4]International Joint Research Centre for Engineering Reliability and Stochastic Mechanics, Tongji University, Shanghai 200092, China

Abstract: The response analysis of the composite structural-acoustic systems with multiple types of epistemic uncertainties is investigated in this paper. Based on the available information for the uncertain parameters, the multiple types of epistemic uncertainties refer to probability-box (p-box) variables, evidence variables and interval variables. The proposed development focused on an efficient computation of the output bounds of the cumulative distribution function of the sound pressure response when

dealing with the combination of p-box variables, evidence variables and interval variables. To reduce the involved computational cost but ensuring the accuracy, all evidence variables and interval variables are transformed into p-box-form variables. Then, a modified interval Monte Carlo method (MIMCM) is developed to estimate the bounds of the cumulative distribution function of the system response. In MIMCM, a sparse Gegenbauer polynomial surrogate model is established with focus on the efficiency and accuracy and then applied for the interval analysis in each iteration. A numerical example and two engineering examples with respect to multiple types of epistemic uncertainties are carried out to illustrate the accuracy and efficiency of the MIMCM by conducting comparisons with traditional algorithms. The ability of the proposed method for risk and conservative reliability analysis is also investigated.

1 Introduction

The noise produced by structural vibration will affect the riding comfort of vehicles, resulting in discomfort of passengers and damage to human health. The analysis of the structural-acoustic coupling system is an important research topic in the field of vibration and noise control. Traditional response analysis of structural-acoustic system is usually carried out in the context of deterministic parameters [1]. However, uncertainties exist in in practical engineering problems inevitably due to manufacturing errors, unpredictable environment, and other factors, which means that unreliable analysis results will be obtained if those uncertain factors are treated as deterministic information. Recently, composite materials have been widely applied in the field of vibration and noise control. As for composite structural-acoustic systems, uncertain

parameters come from two sources. First, at the macro scale, the composite structure-acoustic system is affected by uncertain factors such as geometric size, climatic environment, and external load. Second, at the micro scale, the macroscopic mechanical properties of composite materials fluctuate due to the uncertainty of component materials and microstructure parameters. Thus, the influence of multi-scale uncertainties should be considered in the analysis process of composite structural-acoustic systems in order to obtain an analysis result with valued engineering application.

Uncertainties can be classified into aleatoric uncertainty and epistemic uncertainty according to different natures [2]. Aleatory uncertainty is caused by objective physical conditions and will not be eliminated with the increase of cognitive level, which is usually described by random variables or random processes based on probability theory. Up to now, a number of numerical methods have been developed for dealing with the random system response analysis, such as the Monte Carlo method [3, 4], the perturbation method [5-7], the orthogonal polynomial approximation method [8-10], and so on. However, in practical engineering, the precise probability distribution function (PDF) of uncertain parameters usually cannot be constructed due to the lack of enough probability information. Ben-haim and Elishakoff have reported that even small deviation from the real PDF can lead to large errors of the statistic response [11]. Thus, the analysis of epistemic uncertainty may be more challenging and has greater significance in practical engineering [12].

Epistemic uncertainty is caused by the limitation of cognitive level and insufficient

understanding of objective things. In contrast with aleatory uncertainty, epistemic uncertainty can generally be reduced by additional empirical effort. The probability theory is inappropriate for handling epistemic uncertainties since that the PDF of uncertain parameters are imprecise. Instead, many non-probabilistic theories have been emerged to quantify the epistemic uncertainty, such as interval analysis [13], evidence theory [14], probability box (p-box) [15-20], et al. Epistemic uncertainty model have been applied in many engineering fields, including structure analysis and optimization [21, 22], heat conduction analysis [23], acoustic response analysis [24], brake disc analysis [25] and so on. Some progress on epistemic uncertainty analysis of structural-acoustic system has been made. Xu et al. used statistical energy analysis approach to predict the response of structural-acoustic system with interval parameters [26]. Based on evidence theory, Yin et al proposed a Jacobi-expansion-based approach to predict the response of acoustic system with evidence variables [27]. Based on p-box theory, Chen et al. studied an imprecise probability approach for the uncertain analysis of structural-acoustic system involving p-box variables based on perturbation method [28]. In practical engineering, different types of uncertain parameters may exist simultaneously. Thus, there has been a great interest in developing numerical methods for dealing with engineering problems with hybrid uncertainties [29, 30]. As for structural-acoustic systems, Wang and Huang proposed a polynomial chaos response surface method for uncertainty propagation in structural-acoustic system containing hybrid interval and random parameters [31]. A hybrid evidence theory-based model has been proposed for handling the mixed uncertainties in structural-acoustic systems [32,

33].

From the researches mentioned above, it can be known that many inspiring works have been done in the response analysis of structural-acoustic systems. However, up to now, the uncertain response analysis of composite structural-acoustic system involving p-box variables, evidence variables and interval variables exist simultaneously has not been investigated. This is because this kind of uncertain model is challenging due to the heavy computational burden of the propagation of multiple types of uncertainties. Moreover, the computational cost increased exponentially with the multi-scale uncertain variables involved in the composite structural-acoustic system. In this paper, a modified interval Monte Carlo method (MIMCM) is derived to efficiently deal with this kind of uncertain model. Firstly, the p-box variables, evidence variables and interval variables are transformed into a unified p-box form thereby the interval Monte Carlo method can be applied to calculate the response of the uncertain composite structural-acoustic system. Then, the sparse Gegenbauer polynomial surrogate model is constructed to further reduce the computational cost of repetitive interval analyses in MIMCM. The effectiveness and efficiency of the proposed method is verified by numerical examples.

The remainder of this paper is organized as follows: basic theories for quantifying multiple types of epistemic uncertainties are introduced in Section 2. Then, an evidence-based method for the propagation of multiple types of epistemic uncertainties in composite structural-acoustic system is introduced in Section 3. The modified interval Monte Carlo method is derived for response analysis of composite structural-

acoustic system involving multiple types of epistemic uncertainties in Section 4. One numerical example and two engineering examples are investigated to verify the accuracy and efficiency of the proposed method in Section 5. Finally, conclusion is drawn in Section 6.

2 Representation of multiple types of epistemic uncertainties

2.1 P-box representation

A p-box defines the cumulative distribution function (CDF) F_X of a real-valued random variable X by its lower bound $\underline{F_X}$ and upper bounds $\overline{F_X}$. Let $F_X(x) = P(X \in (-\infty, x]), \forall x \in \Re$, for each x, the CDF $F_X(x)$ is unknown but in a closed interval $[\underline{F_X}(x), \overline{F_X}(x)]$, namely these boundaries form the envelope of the probability family as

$$\Xi = \left\{ P \middle| \forall x \in \Re, \underline{F_X}(x) \le F_X(x) \le \overline{F_X}(x) \right\} \tag{1}$$

Parametric p-boxes and non-parametric p-boxes are two types of p-boxes. Parametric p-boxes are denoted by a family of distribution functions whose parameters lie within an interval, while non-parametric p-boxes are generated by the envelope of true but unknown CDFs [34]. Several methods exist for determining the bounds of a p-box according to different sources of information [34-37].

The convolution algorithm formalized by Ferson et al. [35] can be applied to p-box model. First, a p-box is discretized into a finite list of pairs (A_1, m_1), … (A_n, M_n), where A_i represents an interval, m_i represents the probability mass related to A_i and satisfies $\sum_{i=1}^{n} m_i = 1$. The discretization process of a p-box is shown in Figure 1 [38].

Obviously, the approximate accuracy depends on the detail level of the p-box discretization. Then the uniform discretization is adopted, namely the basic probability assignment m_i is equal to $1/n$, and A_i can be calculated by

$$A_i = \left[\underline{F_X}^{-1}\left(\frac{i-1}{n}\right),\ \overline{F_X}^{-1}\left(\frac{i}{n}\right) \right],\ i = 1, 2, ..., n \tag{2}$$

Where $\underline{F_X}^{-1}$ and $\overline{F_X}^{-1}$ are the inverse function of $\underline{F_X}$ and $\overline{F_X}$ respectively.

Let f: $X \rightarrow Y$ be a mapping and $X=(X_1,X_2)$ be the basic variables modeled by discrete p-boxes which are expressed as

$$\begin{aligned} X_1 &= \{(A_1, m(A_1)), ..., (A_n, m(A_n))\} \\ X_2 &= \{(B_1, m(B_1)), ..., (B_l, m(B_l))\} \end{aligned} \tag{3}$$

In which n and l represent the number of discrete intervals related to X_1 and X_2 respectively.

If X_1 and X_2 are mutually independent, the Cartesian product of $X_1 \times X_2$ can be represented by $\{(R_1, m(R_1)), ..., (R_k,\ m(R_k))\}$, R_k and $m(R_k)$ can be expressed as

$$R_k = A_i \times B_j,\ i = 1, ..., n,\ \ j = 1, ..., l \tag{4}$$

$$m(R_k) = m(A_i) m(B_j) \tag{5}$$

Let $\Re = \{R_k : k = 1, ..., nl\}$, the response quantity Y of mapping f is a discrete p-box can be expressed as

$$\wp = \{ f(R_k) \,|\, R_k \in \Re \} \tag{6}$$

The associated probability assignment m of the focal element $S=f(R_k)$ can be

expressed as

$$m(S) = \sum_{R_k : S = f(R_k)} m(R_k) \tag{7}$$

Let $F_Y(y)$ denote the CDF of response quantity Y, for arbitrary value y, the bounds of $F_Y(y)$ can be calculated by

$$\begin{aligned} \underline{F_Y}(y) &= \sum_{S: y \geq \sup(S)} m(S) \\ \overline{F_Y}(y) &= \sum_{S: y \geq \inf(S)} m(S) \end{aligned} \tag{8}$$

In the above equations, sup(•) and inf(•) represent the supremum and infimum of the function respectively. If the mapping f involves multiple p-box variables, one can employ Eqs. (4)-(7) repeatedly to propagate the p-boxes.

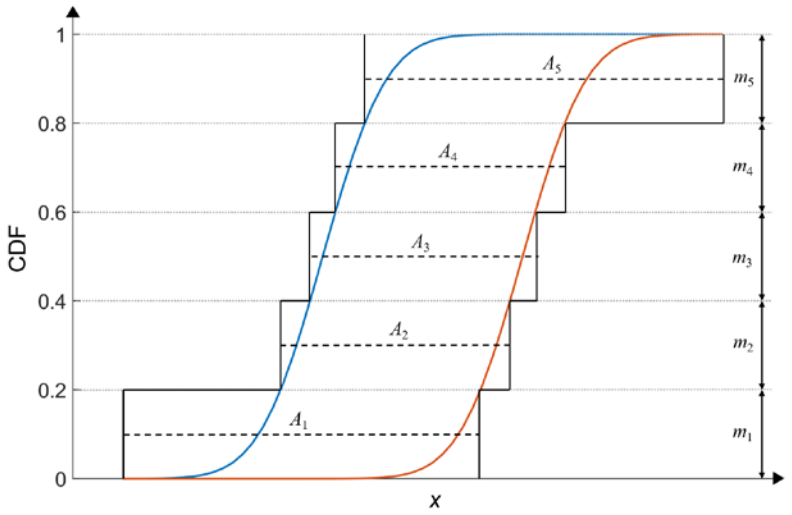

Fig. 1 Discretization of a continuous p-box (n=5)

2.2 Linking p-box with evidence theory and interval

Ref. [35] indicated that the discretized p-box representation can correspond to evidence theory directly. The bounds of p-box according to Eq. (8) are equivalent to

the belief and plausibility measure of evidence theory as shown in Eqs. (9) and (10)

$$\mathrm{Bel}(B) = \sum_{A \subseteq B} m(A) \tag{9}$$

$$\mathrm{Pl}(B) = \sum_{A \cap B \neq \varnothing} m(A) \tag{10}$$

In which, A is a given evidential event. Bel(B) and Pl(B) the lower and upper bounds of probability measure for arbitrary proposition B. $m(A)$ denotes the BPA related to event A. The subset A with $m(A)$ is called the focal element and satisfies

$$\begin{aligned} &m(A) \geq 0, \\ &m(\varnothing) = 0, \\ &\sum m(A) = 1 \end{aligned} \tag{11}$$

Thus, with this specific interpretation, we restrict evidence theory herein to a frequentist basic probability assignment. It can capture all subjectivity, including varying expert inputs, by the topology (size) of the focal elements.

For the case of univariate p-boxes, the focal sets represent intervals. These uncertainties can be processed with interval technologies [13]. An interval vector $\mathbf{X}^I = \left\{ X_1^I, X_2^I, ..., X_L^I \right\}^{\mathrm{T}}$ which consists of L independent variables is expressed as

$$\begin{aligned} &\mathbf{X}^I = \left[\underline{\mathbf{X}}, \overline{\mathbf{X}} \right] = \mathbf{X}^M + \Delta\mathbf{X}^I \\ &\mathbf{X}^M = (\overline{\mathbf{X}} + \underline{\mathbf{X}}) / 2, \ \Delta\mathbf{X}^I = \left[-\Delta\mathbf{X}, \Delta\mathbf{X} \right], \ \Delta\mathbf{X} = (\overline{\mathbf{X}} - \underline{\mathbf{X}}) / 2 \end{aligned} \tag{12}$$

In which $\underline{\mathbf{X}}$ and $\overline{\mathbf{X}}$ are the lower and upper bounds of $\mathbf{X}^I$ respectively. $\mathbf{X}^M$ represents the midpoint of $\mathbf{X}^I$. $\Delta\mathbf{X}^I$ and $\Delta\mathbf{X}$ represent the deviation interval and the maximum deviation of $\mathbf{X}^I$ respectively.

3 Propagation of multiple types of epistemic uncertainties in composite structural-acoustic system

3.1 Uncertain FEM model of the composite structural-acoustic system

The dynamic equilibrium equation of the composite structural-acoustic system is expressed as [39]

$$\begin{gathered}\mathbf{ZU} = \mathbf{F},\\ \mathbf{Z} = \begin{bmatrix} \mathbf{K}_s + i\omega\mathbf{C}_s - \omega^2\mathbf{M}_s & -\mathbf{H} \\ \rho_f \omega^2 \mathbf{H}^T & \mathbf{K}_f - \omega^2\mathbf{M}_f \end{bmatrix},\\ \mathbf{U} = \left\{\mathbf{u}_s \ \ \mathbf{p}\right\}^T,\ \mathbf{F} = \left\{\mathbf{F}_b \ \ \mathbf{F}_q\right\}^T\end{gathered} \tag{13}$$

Where $\mathbf{K}_s$ and $\mathbf{M}_s$ are stiffness matrix and mass matrix of the composite structure, and $\mathbf{C}_s$ is the damping matrix. ω denotes the angular frequency of the external excitation. $\mathbf{H}$ denotes the spatial coupling matrix. ρ_f is the density of the acoustic field. $\mathbf{u}_s$ represents the displacement vector of the composite structure. $\mathbf{p}$ is the sound pressure vector of the acoustic field. $\mathbf{F}_s$ and $\mathbf{F}_f$ represents the generalized force vectors associated with the composite structure and the internal acoustic field, respectively.

$\mathbf{K}_s$ and $\mathbf{M}_s$ and $\mathbf{C}_s$ can be represented as

$$\mathbf{K}_s = \sum_{j=1}^{N_{cell}} \int_{\Omega_j} \mathbf{B}^{\mathrm{T}} \mathbf{D}^{\mathrm{H}} \mathbf{B} d\Omega \tag{14}$$

$$\mathbf{M}_s = \sum_{j=1}^{N_{cell}} \int_{\Omega_j} \eta^{\mathrm{H}} \mathbf{N}_{\mathrm{s}}^{\mathrm{T}} \mathbf{N}_{\mathrm{s}} d\Omega \tag{15}$$

$$\mathbf{C}_s = \alpha\mathbf{M}_s + \beta\mathbf{K}_s \tag{16}$$

In which $\mathbf{B}$ represents the strain matrix at the macroscale. $\mathbf{D}^{\mathrm{H}}$ is the equivalent

macro constitutive matrix of composite microstructure and the detailed can be found in Ref [39]. $\mathbf{N}_s$ is the Lagrange shape function of the isoperimetric quadrilateral element. Ω_j and N_{cell} denotes the jth element and the total number of elements in the domain. α and β represents the damping coefficients of the damping material.

$\mathbf{K}_f$ and $\mathbf{M}_f$ can be obtained by

$$\mathbf{K}_f = \sum_{e=1}^{n_{cell}} \int_{\Omega_e} \left(\nabla \mathbf{N}_f\right)^{\mathrm{T}} \left(\nabla \mathbf{N}_f\right) \mathrm{d}\Omega \tag{17}$$

$$\mathbf{M}_f = \sum_{e=1}^{n_{cell}} \frac{1}{c^2} \int_{\Omega_e} \mathbf{N}_f^{\mathrm{T}} \mathbf{N}_f \mathrm{d}\Omega \tag{18}$$

Where $\mathbf{N}_f$ is the Lagrange shape function of the isoperimetric hexahedral element. Ω_e and n_{cell} denotes the eth element and the total number of elements in the acoustic domain.

Let $\mathbf{x}$ represents the uncertain parameter vector in the composite structural-acoustic system. All the variables are assumed to be independent in this paper. By introducing the uncertain parameter vector $\mathbf{x}$, the dynamic equilibrium equation of the composite structural-acoustic system shown in Eq. (13) can be rewritten as

$$\mathbf{Z}(\mathbf{x})\mathbf{U}(\mathbf{x}) = \mathbf{F}(\mathbf{x}) \tag{19}$$

In which $\mathbf{Z}(\mathbf{x})$, $\mathbf{U}(\mathbf{x})$and $\mathbf{F}(\mathbf{x})$ and represent the uncertain composite structural-acoustic dynamic stiffness matrix, uncertain frequency response vector and the uncertain excitation vector, respectively.

3.2 Hybrid discrete method (HDM) for composite structural-acoustic model with multiple types of uncertainties

In practical engineering, three types of epistemic uncertainties mentioned above may exist in composite structure-acoustic system simultaneously. As mentioned above, p-box model can be transformed to evidence model by using convolution algorithm, and the interval model can bet treated as evidence model with only one focal element. Then **x** can be transformed into a pure evidence variables vector

$$\mathbf{x} = [\mathbf{x}_{L_1}, \mathbf{x}_{L_2}, \mathbf{x}_{L_3}] = [x_1, x_2, ..., x_{L_1}, x_{L_1+1}, ..., x_{L_1+L_2}, x_{L_1+L_2+1}, ..., x_{L_1+L_2+L_3}] \tag{20}$$

Where L_1 and L_3 denote the number of transformed p-box variables and interval variables, respectively. L_2 denote the number of evidence variables.

Thus, the uncertain composite structural-acoustic system model established by (19) turn into a pure evidence theory uncertain model. Here, an evidence-theory-based method named as hybrid discrete method (HDM) is applied to calculate the uncertain model and briefly introduced below.

The joint FD for evidence variables vector **x** is denoted as **S** and can be defined by using the Cartesian product as following

$$\mathbf{S} = x_1 \times x_2 \times ... \times x_L = \left\{ \mathbf{s}_k = \left[u_1, u_2, ..., u_L \right], u_j \in x_j,\ j = 1, 2, ..., L, k = 1, 2, ..., n_s \right\} \tag{21}$$

Where $\mathbf{s}_k$ represented the focal element of the joint FD. u_j is the focal element of x_j. Assuming that the number of focal elements for the jth evidence variable is l_j (j=1,2, …, L), the total number of $\mathbf{s}_k$ is $n_s = l_1 \times l_2 \times \ldots \times l_L$. In this paper, x_j is considered as a

continuous interval, and the joint BPA for $\mathbf{s}_k$ can be calculated by

$$m_s(\mathbf{s}_k) = \begin{cases} \prod_{j=1}^{L} m(u_j), u_j \in \mathbf{s}_k \\ 0, else. \end{cases} \tag{22}$$

Then the response **U(x)** for each joint focal element $\mathbf{s}_k$ can be represented by an interval with its corresponding BPA and expressed as

$$\begin{aligned} Y_{\mathbf{s}_k}^{\mathrm{I}} &= \left[\underline{Y_{\mathbf{s}_k}}, \overline{Y_{\mathbf{s}_k}}\right] = \left[\min_{\mathbf{x}\in\mathbf{s}_k} \mathbf{U}, \max_{\mathbf{x}\in\mathbf{s}_k} \mathbf{U}\right]. \\ m_Y(Y_{\mathbf{s}_k}^{\mathrm{I}}) &= \begin{cases} m(\mathbf{s}_k) \\ 0, else. \end{cases} \end{aligned} \tag{23}$$

Where $m_Y(Y_{\mathbf{s}_k}^{\mathrm{I}})$ denotes the BPA for $Y_{\mathbf{s}_k}^{\mathrm{I}}$. $Y_{\mathbf{s}_k}^{\mathrm{I}}$ can be obtained by several interval algorithms, i.e. the Monte Carlo method, the interval perturbation method and so on, then the Bel and Pl of **U(x)** can be calculated through Eqs. (9) and (10).

4 Modified interval Monte Carlo method (MIMCM) for analysis of composite structural-acoustic system involving multiple types of epistemic uncertainties

The main disadvantage of the HDM is the full factorial design. The number of total focal elements from the Cartesian products increases exponentially with the number of uncertain variables. As for high-dimensional imprecise problems， the computation cost of HDM is prohibitive due to the combinatorial explosion [35]. Interval Monte Carlo method (IMCM) is an effective method to overcome the shortcoming of the Cartesian product [40]. By extending the IMCM, a modified interval Monte Carlo method (MIMCM) is derived for response analysis of composite

structural-acoustic system involving multiple types of epistemic uncertainties in this section.

4.1 Unification of multiple types of epistemic uncertainties

The evidence variables and interval variables need to be transformed into p-box form due to IMCM is applied to the case with only p-box variables. For an evidence variable *E* which can be specified by its focal elements and their associated probability masses $\left\{\left(\left[a_1, b_1\right], m_1\right), ..., \left(\left[a_n, b_n\right], m_n\right)\right\}, \sum m_i = 1, i = 1, ..., n$, an associated p-box can always be obtained from *E* and the bounds of it can be obtained by [35]

$$\begin{aligned} \overline{F_E}(e) &= \sum_{a_i \le e} m_i \\ \underline{F_E}(e) &= \sum_{b_i < e} m_i \end{aligned} \tag{24}$$

In which $\overline{F_E}(e)$ and $\underline{F_E}(e)$ are the cumulative plausibility function and the cumulative belief function for *E* respectively. Such a pair of functions define a p-box because they are nondecreasing from reals into the interval [0, 1] and $\underline{F_E}(e)$ is always less than or equal to $\overline{F_E}(e)$ for every value of *e*.

As for an interval variable, lower and upper bounds of it are already given. Thus, the interval variable can be simply treated as an evidence variable who has just one focal element and its associated probability mass been equal to 1. Then the bounds of the associate p-box of the interval variable can be directly obtained through Eq. (24)

4.2 Uncertainty propagation of p-boxes using IMCM

In the first step, the interval transform method is applied to generate the intervals in accordance with the prescribed p-boxes. The generation process is graphically

demonstrated in Figure 2 for one-dimensional case and follows the steps outlined below: Firstly, a standard uniform random number u_k (k=1, 2, …, n) is generated. Then the intersection of a line of u_k and the CDF of p-box variable will generate an interval set $\boldsymbol{x} = \left\{ \left[\underline{x_1}, \overline{x_1} \right], ..., \left[\underline{x_n}, \overline{x_n} \right] \right\}$. For arbitrary u_k, the corresponding interval $\left[\underline{x_k}, \overline{x_k} \right]$ (k=1,2,…,n) contains all possible simulated numbers from the ensemble of distributions for u_k. Thus, the set of intervals $\left\{ \left[\underline{x_1}, \overline{x_1} \right], ..., \left[\underline{x_n}, \overline{x_n} \right] \right\}$ is the sample consistent with the original p-box, where n denotes the total number of u_k. For uncertain system involving L p-box variables, the standard uniform random vector $\boldsymbol{u}_k = [u_{k,1}, u_{k,2}, ..., u_{k,L}]$ (k=1,2,…,n) should to be firstly generated, then the intervals $\left[\underline{x_{k,q}}, \overline{x_{k,q}} \right]$ (q=1,2,…,n) can be generated through the intersections of lines of $u_{k,q}$ with the bounds defining the p-boxes for each p-box variable.

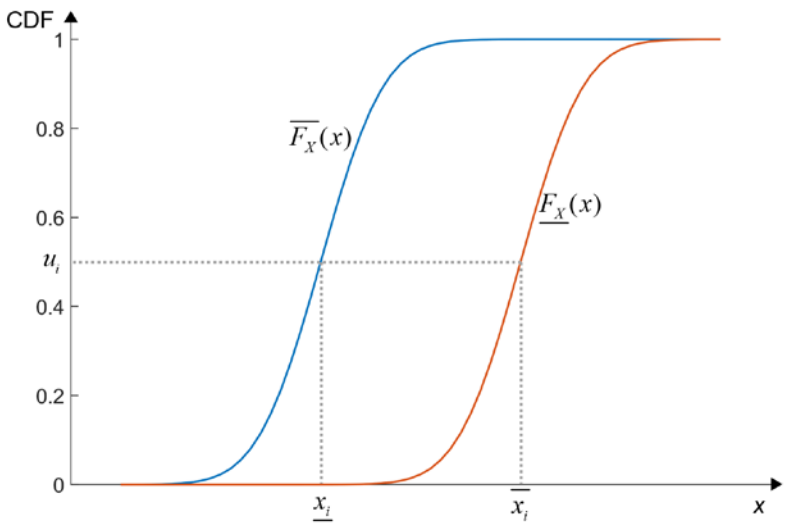

Fig. 2 Generation process of random intervals

In the second step, based on the randomly generated intervals, the interval responses of composite structural-acoustic system in each iteration can be calculated through the interval algorithm and expressed as $\boldsymbol{U}_k^{\mathrm{I}}$ (k=1,2, …, n), where

$U_k^{\mathrm{I}} = \left[\underline{U}_k, \overline{U}_k\right]$. U_k^{I} can be regarded as a discrete p-box and its associated probability assignment is 1/*n*.

Finally, the left and right cumulative distribution function boundary of the response of composite structural-composite system **U** can be calculated through the following steps: (1)Get a response set U_j (j=0,1,…,2n) by sorting the $\underline{U_k}$ and $\overline{U_k}$ from smallest to largest; (2) Get the left and right cumulative distribution function boundary of the response **U** by following equations

$$\begin{aligned} \underline{F_{\mathbf{U}}} &= \sum_{\overline{U_k} \le U_j} 1/n \\ \overline{F_{\mathbf{U}}} &= \sum_{\underline{U_k} \le U_j} 1/n \end{aligned} \tag{25}$$

4.3 Sparse Gegenbauer polynomial surrogate model (SGPSM) for interval analysis in IMCM

As mentioned above, the second step of IMCM consists of at least thousands of interval analysis, which means the computational efficiency of the interval analysis is important. Of great interest here is to use surrogate model to reduce the computational burden caused by the recalculation of interval responses. As the uncertain parameter is always bounded in practical uncertain systems, the orthogonal polynomial is a suitable choice to construct the surrogate model with comprehensive consideration of accuracy and efficiency. It should be noted that many orthogonal polynomials can be adopted to calculate the interval responses of uncertain systems, such as the Chebyshev polynomial [41], the Gegenbauer polynomial [42] and the Jacobi polynomial [27]. All these orthogonal polynomials can achieve good accuracy for interval analysis. In this

paper, the Gegenbauer polynomial is chose due to its convenience in choice of polynomial parameter and linear conversion of arbitrary interval variable. The foundation of Gegenbauer polynomial is briefly introduced in Appendix.

As shown in Eq. (59) in appendix, the number of interpolation points will keep growing exponentially as the number of uncertain variables and the retained order increase, which means the computation burden for the construction of the Gegenbauer polynomial surrogate model will be heavy when dealing with multiple variables. Thus, the sparse sampling technique is introduced to improve the efficiency of constructing the Gegenbauer polynomial surrogate model. The sparse Gegenbauer polynomial surrogate model (SGPSM) of composite structural-acoustic system for interval analysis in IMCM is derived below.

4.3.1 The expression of SGPSM

The interpolation points $\hat{\xi}_j^{\lambda}(j=1,2,...,m)$ of each variable in Gegenbauer polynomial are the roots of $G_m^{\lambda}(\xi)$, where m is the total number of interpolation points. The interpolation points are symmetrical with respect to zero. These interpolation points form the candidate samples $\boldsymbol{\xi}$ set. The premise condition of sequential sampling is that the sampling points are uniformly chosen from the uniform candidate set, but the interpolation points are not uniformly distributed and are denser around the bounds of the interval space. Therefore, a weight number set $\boldsymbol{\beta}$ space is introduced to treat the non-equidistant interpolation points as sampling points with the same weight.

The candidates of the $\boldsymbol{\xi}$ set and the $\boldsymbol{\beta}$ space can be obtained through tensor product

operation and represented as

$$\boldsymbol{\xi} = \boldsymbol{\xi}_1 \otimes \cdots \otimes \boldsymbol{\xi}_L, \qquad \boldsymbol{\beta} = \boldsymbol{\beta}_1 \otimes \cdots \otimes \boldsymbol{\beta}_L \tag{26}$$

in which $\boldsymbol{\xi}_i$ and $\boldsymbol{\beta}_i$ denote the candidates of ith variable in the $\boldsymbol{\xi}$ set and $\boldsymbol{\beta}$ space.

m is determined by the highest allowable order $n_{\max}$ of the Gegenbauer surrogate model and set as $m = n_{\max} + 1$ in order to balance the accuracy and efficiency. $n_{\max}$ is determined by the largest allowable sampling size $N_{\max}$ which should be larger than the number of coefficients N_C and expressed as

$$N_C(n_{\max}, L) = \frac{(L + n_{\max})!}{L!\, n_{\max}!} < N_{\max} \tag{27}$$

Thus, the number of candidate samples for L-dimensional surrogate model is $(n_{\max}+1)^L$. After determining m, the number of candidate samples remains unchanged, then this fixed sample candidate set is adopted for any order n, which means the sampling efficiency can be greatly improving. Then the samples in candidate set can be uniformly sorted by using the scalar-valued criterion function [43] and represented as

$$\phi_q(\boldsymbol{\beta}) = \left(\sum_{i=1}^{s_0} \sum_{j=i+1}^{s_0} d\left(\boldsymbol{\beta}^{(i)}, \boldsymbol{\beta}^{(j)}\right)^{-q} \right)^{1/q} \tag{28}$$

In which q represents a relative larger integer, which is taken as 100 in this paper. $\boldsymbol{\beta}^{(i)}$ denotes a sampling candidate space in the $\boldsymbol{\beta}$ space, s_0 is the number of samples. $d(\boldsymbol{\beta}^{(i)}, \boldsymbol{\beta}^{(j)})$ denotes a Euclidean distance and is defined as

$$d\left(\boldsymbol{\beta}^{(i)}, \boldsymbol{\beta}^{(j)}\right) = \left(\sum_{k=1}^{L} \left| \beta_k^{(i)} - \beta_k^{(j)} \right|^2 \right)^{1/2} \tag{29}$$

Where $\beta_k^{(i)}$ is the kth variable of the L-dimensional $\boldsymbol{\beta}^{(i)}$.

A smaller ϕ_q means a more evenly extraction of sampling points. To implement the sampling scheme, the initial sampling points must be obtained. The number of initial sampling points is $N_0=mL$. The initial sampling points can be written by a matrix whose column and row denote a sequence of variables and sampling points, respectively. To yield the highest uniformity of the sampling points, the first m elements of the first row and all elements of the first column are set as uniform. Set the first m elements of the first row as 1,2, …, m. Set the ith dimension of the first column as i. If i is bigger than m, the ith dimension is set as the remainder of i/m. The new sample points are sequentially selected by minimizing ϕ_q. The selected sampling set and the rest of the candidate set is denoted as $\boldsymbol{\beta}$ and $\boldsymbol{\delta}$, respectively.

New sampling points from the rest candidate set $\boldsymbol{\delta}$ are added to the selected sampling set $\boldsymbol{\beta}$. The new sample set $\left(\boldsymbol{\beta},\boldsymbol{\beta}_1^{(j)}\right)$ consists of the old $\boldsymbol{\beta}_0^{(i)}\in\boldsymbol{\beta}$ and the new sampling points $\boldsymbol{\beta}_1^{(j)}\in\boldsymbol{\delta}$. The subscript 0 and superscript (i) represent the old sampled set and the ith sample of $\boldsymbol{\beta}$, respectively. The subscript 1 and superscript (j) represent the new sampled set and the jth sample of the $\boldsymbol{\delta}$. The ϕ_q of new sample set can be obtained by

$$\begin{aligned}\phi_q\left(\boldsymbol{\beta},\boldsymbol{\beta}_1^{(j)}\right)&=\left(\sum_{i_1=1}^{s_0}\sum_{i_2=i+1}^{s_0}d\left(\boldsymbol{\beta}_0^{(i_1)},\boldsymbol{\beta}_0^{(i_2)}\right)^{-q}+\sum_{i_1=1}^{s_0}d\left(\boldsymbol{\beta}_0^{(i_1)},\boldsymbol{\beta}_1^{(j)}\right)^{-q}\right)^{1/q}\\&=\left(\phi_q\left(\boldsymbol{\beta}\right)+\sum_{i_1=1}^{s_0}d\left(\boldsymbol{\beta}_0^{(i_1)},\boldsymbol{\beta}_1^{(j)}\right)^{-q}\right)^{1/q}\end{aligned}\tag{30}$$

Sequentially substituting the points of $\boldsymbol{\delta}$ into Eq. (30) to calculate the ϕ_q, where

the sampling point with the minimum value of ϕ_q will be selected into the set $\boldsymbol{\beta}$ as a new sample point.

The first term on the right-hand side in Eq. (30) is a constant, which means the order of ϕ_q calculated after removing the first term is the same as before. Thus, the Eq. (30) can be simplified as following

$$\phi_q\left(\boldsymbol{\beta},\boldsymbol{\beta}_1^{(j)}\right)=\left(\sum_{i_1=1}^{s_0} d\left(\boldsymbol{\beta}_0^{(i_1)},\boldsymbol{\beta}_1^{(j)}\right)^{-q}\right)^{1/q} \tag{31}$$

When the first m columns are determined, the other columns also can be determined by repeating this update process, after all dimensions are uniformed, the sampling process in done. More detailed information can be found in literature [44].

By using the sequential sampling scheme, a L-dimensional function $f(\boldsymbol{\xi})$ defined on $\boldsymbol{\xi}\in[-1,1]$ can be approximated by Gegenbauer polynomials as

$$f(\boldsymbol{\xi})=\hat{f}(\boldsymbol{\xi})=\sum_{0\le i_1+\cdots+i_L\le n_{\max}} f_{i_1,\ldots,i_L} G_{i_1,\ldots,i_L}^{\lambda_1,\ldots,\lambda_L}(\boldsymbol{\xi}),\ i_1,\ldots,i_L=0,1,\ldots,n_{\max}. \tag{32}$$

The number of the Gegenbauer polynomials can be reduced from $N_{\text{total}} = (N_1+1) \times (N_2+1) \times \cdots \times (N_L+1)$ to a small sum [44]

$$N_{\text{C}}(n_{\max},L)=\frac{(L+n_{\max})!}{L!n_{\max}!}. \tag{33}$$

Where $n_{\max}$ is the highest allowable order of the Gegenbauer polynomial.

Obviously, the computational burden of coefficients calculation is reduced, thus the efficiency of the high-order Gegenbauer polynomial will significantly improving in

dealing with multi-dimensional problems.

Then the least squares method can be used to obtain the coefficients of the Gegenbauer polynomials [44]. Then the Eq. (32) can be transformed as

$$\hat{f}(\boldsymbol{\xi}) = \sum_{0 \le i_1 + \cdots + i_L \le n_{\max}} f_{i_1,\ldots,i_L} G_{i_1,\ldots,i_L}^{\lambda_1,\ldots,\lambda_L}(\boldsymbol{\xi}) = \boldsymbol{\eta}^{\mathrm{T}} \boldsymbol{\alpha} \tag{34}$$

In which $\boldsymbol{\eta}$ and $\boldsymbol{\alpha}$ denote the coefficient vector and the polynomial basis vector respectively, which can be expressed as

$$\boldsymbol{\eta} = [\eta_1 \cdots \eta_s]^{\mathrm{T}} = [f_{0,\ldots,0} \cdots f_{i_1,\ldots,i_L}]^{\mathrm{T}}, 0 \le i_1 + \cdots + i_L \le n_{\max} \tag{35}$$

$$\boldsymbol{\alpha} = [\alpha_1 \cdots \alpha_s]^{\mathrm{T}} = [G_{0,\ldots,0} \cdots G_{i_1,\ldots,i_L}]^{\mathrm{T}}, 0 \le i_1 + \cdots + i_L \le n_{\max} \tag{36}$$

Where s represents the number of coefficients in $\boldsymbol{\eta}$ and the number of Gegenbauer polynomials in $\boldsymbol{\alpha}$. According to Eq. (33), $s=N_{\mathrm{C}}$.

$\boldsymbol{\eta}$ can be obtained through the least squares method and expressed as follow

$$\boldsymbol{\eta} = (\mathbf{A}^{\mathrm{T}}\mathbf{A})^{-1}\mathbf{A}^{\mathrm{T}}\mathbf{Y} \tag{37}$$

In which

$$\mathbf{Y} = \left[f(\hat{\xi}_1) \cdots f(\hat{\xi}_s) \right]^{\mathrm{T}}, \quad s = N_{\mathrm{C}} \tag{38}$$

$$\mathbf{A} = \begin{bmatrix} \alpha_1(\hat{\xi}_1) & \cdots & \alpha_s(\hat{\xi}_1) \\ \vdots & \ddots & \vdots \\ \alpha_s(\hat{\xi}_s) & \cdots & \alpha_s(\hat{\xi}_s) \end{bmatrix}, \quad s = N_{\mathrm{C}} \tag{39}$$

In the above equations, $\hat{\xi}_1,\ldots,\hat{\xi}_s$ are the sparse sampling points. The vector $\mathbf{Y}$ denotes the value of the original function at the sampling points, the matrix $\mathbf{A}$ consists of the polynomial basis vectors at the sampling points.

4.3.2 SGPSM of composite structural-acoustic system for interval analysis

Consider the composite structural-acoustic system involving L independent multiple variables, the uncertain variable vector can be expressed as

$$\mathbf{p} = \left[p_1, ..., p_{L_1}, ..., p_{L_1+L_2}, ..., p_{L_1+L_2+L_3} \right] \tag{40}$$

In which L_1, L_2 and L_3 represent the number of p-boxes variables, evidence variables and interval variables respectively, and L_1+ L_2 +L_3= L. In practical engineering, these uncertain parameters are always bounded, then Eq. (40) can be rewritten as

$$\begin{aligned} &\mathbf{p}^{\mathrm{I}} = \left[p_1^{\mathrm{I}}, p_2^{\mathrm{I}}, ..., p_L^{\mathrm{I}} \right], \\ &p_q^{\mathrm{I}} = \left[\underline{p_q}, \overline{p_q} \right], q = 1, 2, ..., L \end{aligned} \tag{41}$$

The Gegenbauer polynomial can be directly applied for interval analysis by using a transformation process [42]. The arbitrary interval vector $\mathbf{p}^{\mathrm{I}}$ can be transformed as a function of interval vector $\boldsymbol{\xi}^{\mathrm{I}}$ defined on [-1,1], which can be expressed as

$$\begin{aligned} &\mathbf{p}^{\mathrm{I}} = \mathbf{p}^{\mathrm{I}}(\boldsymbol{\xi}^{\mathrm{I}}), \quad \boldsymbol{\xi}^{\mathrm{I}} = \left[\xi_1^{\mathrm{I}}, \xi_2^{\mathrm{I}}, ..., \xi_L^{\mathrm{I}} \right], \\ &p_q^{\mathrm{I}} = p_q^{\mathrm{I}}(\xi_q^{\mathrm{I}}) = m_q + d_q \xi_q^{\mathrm{I}}, \quad q = 1, 2, ..., L \end{aligned} \tag{42}$$

In which

$$m_q = \frac{\overline{p_q} + \underline{p_q}}{2}, \qquad d_q = \frac{\overline{p_q} - \underline{p_q}}{2} \tag{43}$$

The accuracy of Gegenbauer polynomials for interval model increases as the value of polynomial parameter λ decrease [42]. Therefore, the parameter λ_i of Gegenbauer polynomials related to interval variables is given as λ_i = 0.001 and marked as λ^0 in this paper.

Thus, the response of composite structural-acoustic system **U** can be approximated through SGPSM by

$$\mathbf{U} = \mathbf{U}(\mathbf{p}^{\mathrm{I}}) \approx \tilde{\mathbf{U}}(\boldsymbol{\xi}^{\mathrm{I}}) = \sum_{0 \le i_1 + \cdots + i_L \le n_{\max}} f_{i_1,\ldots,i_L} G_{i_1,\ldots,i_L}^{\lambda_0,\ldots,\lambda_0}(\boldsymbol{\xi}^{\mathrm{I}}) = \boldsymbol{\eta}^{\mathrm{T}} \boldsymbol{\alpha}^{\lambda_0} \tag{44}$$

The $\boldsymbol{\eta}$ and $\boldsymbol{\alpha}^{\lambda_0}$ can be obtained through Eqs. (37)-(39) and Eq. (36).

Then by going through the first step in IMCM shown in section 4.2, the hybrid interval set $\mathbf{p}_k^{\mathrm{I}}$ in the *k*th iteration can be expressed as

$$\begin{aligned} &\mathbf{p}_k^{\mathrm{I}} = \left\{ p_{k,1}^{\mathrm{I}}, p_{k,2}^{\mathrm{I}}, \ldots, p_{k,L}^{\mathrm{I}} \right\}, \ k = 1,2,\ldots n \\ &p_{k,q}^{\mathrm{I}} = \left[\underline{p_{k,q}}, \overline{p_{k,q}} \right], \quad q = 1,2,\ldots,L \end{aligned} \tag{45}$$

In which *n* is the total number of iterations of IMCM, namely the sample size.

It should be pointed out that $\mathbf{p}_k^{\mathrm{I}} \subseteq \mathbf{p}^{\mathrm{I}}$, namely the SGPSM constructed through Eq. (44) can be directly employed in interval analysis of each iteration. Similarly, the interval vector $\mathbf{p}_k^{\mathrm{I}}$ related to the *k*th iteration should be transformed as functions of $\boldsymbol{\theta}_k^{\mathrm{I}} \subseteq \boldsymbol{\xi}^{\mathrm{I}} \in [-1,1]$ and expressed as

$$\begin{aligned} &\mathbf{p}_k^{\mathrm{I}} = \mathbf{p}_k^{\mathrm{I}}(\boldsymbol{\theta}_k^{\mathrm{I}}), \quad \boldsymbol{\theta}_k^{\mathrm{I}} = \left[\theta_{k,1}^{\mathrm{I}}, \theta_{k,2}^{\mathrm{I}}, \ldots, \theta_{k,L}^{\mathrm{I}} \right], \\ &p_{k,q}^{\mathrm{I}} = p_{k,q}^{\mathrm{I}}(\theta_{k,q}^{\mathrm{I}}) = m_{k,q} + d_{k,q}\theta_{k,1}^{\mathrm{I}}, \quad q = 1,2,\ldots,L \end{aligned} \tag{46}$$

Where

$$m_{k,q} = m_q = \frac{\overline{p_q} + \underline{p_q}}{2}, \qquad d_{k,q} = d_q = \frac{\overline{p_q} - \underline{p_q}}{2} \tag{47}$$

Then the lower and upper bounds of response U_k^{I} in the *k*th iteration can be evaluated by the following equations

$$\begin{aligned}
\underline{U_k} &= \underline{\tilde{U}(\boldsymbol{\theta}_k^{\mathrm{I}})} = \min_{\boldsymbol{\theta}_k^{\mathrm{I}} \in [-1,1]} \left\{ \sum_{0 \le i_1 + \cdots + i_L \le n_{\max}} f_{i_1,\ldots,i_L} G_{i_1,\ldots,i_L}^{\lambda_0,\ldots,\lambda_0}(\boldsymbol{\theta}_k^{\mathrm{I}}) \right\} \\
\overline{U_k} &= \overline{\tilde{U}(\boldsymbol{\theta}_k^{\mathrm{I}})} = \max_{\boldsymbol{\theta}_k^{\mathrm{I}} \in [-1,1]} \left\{ \sum_{0 \le i_1 + \cdots + i_L \le n_{\max}} f_{i_1,\ldots,i_L} G_{i_1,\ldots,i_L}^{\lambda_0,\ldots,\lambda_0}(\boldsymbol{\theta}_k^{\mathrm{I}}) \right\}, \quad i_1,\ldots,i_L = 0,\ldots,n_{\max}
\end{aligned} \tag{48}$$

Note that the lower and upper bounds of U_k^{I} are simple functions which can be efficiently calculated. In this paper, the Monte Carlo Simulation is adopted to calculate the extreme value of the functions in Eq. (48). It should be pointed out the SGPSM is the same in each iteration once the bounds of the unified form uncertain variables are obtained, which means the SGPSM is only need to be constructed once and thereby the efficiency is good.

The steps of constructing the SGPSM of composite structural-acoustic system for interval analysis can be concluded as following:

Step1. Input p-box variables $\mathbf{a} = \left[a_1, \ldots, a_{L_1} \right]$, evidence variables $\mathbf{b} = \left[b_1, \ldots, b_{L_2} \right]$, interval variables $\mathbf{c} = \left[c_1, \ldots, c_{L_3} \right]$

Step2. Transform hybrid variables into unified p-box form uncertain vector by Eq.(24), whose bound vector is $\mathbf{p}^{\mathrm{I}} = \left[p_1^{\mathrm{I}}, \ldots, p_{L_1}^{\mathrm{I}}, \ldots, p_{L_1+L_2}^{\mathrm{I}}, \ldots, p_{L_1+L_2+L_3}^{\mathrm{I}} \right]$, $L_1+L_2+L_3=L$.

Step3. Calculate the transformation coefficients m_q and d_q of $\mathbf{p}^{\mathrm{I}}$ by Eq. (47), q=1,2,…,L.

Step4. Produce sparse sampling points $\tilde{\xi}_s$ (s=1,2,…,N_{C}), calculate the response $\mathbf{Y}$ and the polynomial basis $\mathbf{A}$ at the sampling points through Eqs. (38) and (39).

Step5. Calculate the coefficients $f_{i_1,\ldots,i_L}$ of Gegenbauer polynomials by Eq. (37), construct the Gegenbauer expansion $\tilde{\mathbf{U}}(\boldsymbol{\xi}^{\mathrm{I}})$ for the approximation of original interval response $\mathbf{U}(\mathbf{p}^{\mathrm{I}})$,namely SGPSM.

4.4 Procedure of MIMCM

To sum up, the proposed MIMCM has made the following developments: Firstly, evidence variables and interval variables are transformed into p-box-form variables thereby IMCM can be applied to handle multiple types of epistemic uncertainties. Secondly, the sparse Gegenbauer polynomial surrogate model is developed to obtain the interval response of composite structural-acoustic system in each iteration, which can greatly improve the calculation efficiency of IMCM.

The detailed procedure of proposed MIMCM for response analysis of composite structural-acoustic system with multiple types of epistemic uncertainties can be expressed by a flow chart shown as Figure 3.

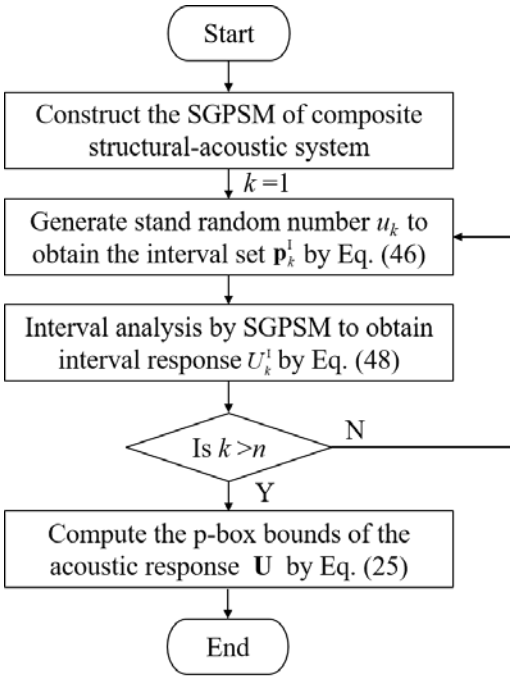

Fig. 3 Flowchart of the proposed MIMCM

5 Numerical examples and discussions

In this section, one numerical example and two engineering examples are considered to verify the performance of the MIMCM. All the simulations are carried out by using MATLAB R2015b on a 3.30GHz Intel(R) Xeon(R) CPU E3-1230 V2.

5.1 A nonlinear function

In this subsection, a simple nonlinear function is applied to verify the accuracy and efficiency of the proposed MIMCM. For brevity, the function is defined as

$$y = \arctan x_1 + \frac{2x_1}{x_2^2} + x_3 x_4 + x_5 x_6^{x_3} + \frac{3^{x_1}}{x_5 x_6} \tag{49}$$

In which x_i (i=1,…,6) are defined as dimensionless variables. Among these variables, x_1, x_2 ,x_3 are assumed as p-box variables and their range variation are [2.7, 3.3], [3.6, 4.4] and [0.9, 1.1], respectively. x_4 is assumed as evidence varible and its range variation is [1.8, 2.2]. x_5 and x_6 are assumed as interval variables and their range variation are [4.5, 5.5] and [5.4, 6.6], respectively. The detail probabilistic information of each variable is listed in Table 1.

Table 1 The distribution type and probabilistic information of variables

Variable	Distribution	Probabilistic information				
x_1	Uniform	Parameter $a \in [2.7, 3]$		Parameter $b \in [3, 3.3]$		
x_2	Gaussian	Mean $\mu \in [3.69, 4.31]$		Standard deviation σ =0.03		
x_3	Non-parametric	$\overline{F}_X = 266.66x^3-837.13x^2+876.6x-305.2582$		$\underline{F}_X = 333.34x^3-964.28x^2+930.2x-299.118$		
x_4	Evidence	*Interval*	[1.8, 1.9]	[1.9, 2.0]	[2.0, 2.1]	[2.1, 2.2]
		BPA	0.1	0.2	0.3	0.4

x_5	Interval	*None*
x_6	Interval	*None*

Here, the results obtained by the hybrid discrete method (HDM) is used as reference solutions. In HDM, the MCS is employed for the interval analysis with respect to each joint focal element. In order to guarantee the accuracy, the sampling number in MCS is set to be 10000 and the p-box variables are discretized into a finite list of 100 pairs. With combination of the evidence variable, the number of the focal elements of joint FD is 4×10^6 in HDM. In MIMCM, the retained order related to each variable in SGPSM is 3 when the precision is satisfied. This means that the nonlinear function should be called for N_C=84 times to construct the SGPSM. In MIMCM, the sample size of the standard uniform random number is set as 5000 after investigating the convergence of MIMCM. The upper bound (UB) and lower bound (LB) of the CDF of the function response y calculated by HDM and MIMCM are shown in Figure 4. Besides, the relative error (RE) of the bounds of y calculated by MIMCM and HDM corresponding to different CDF values are listed in Table 2.

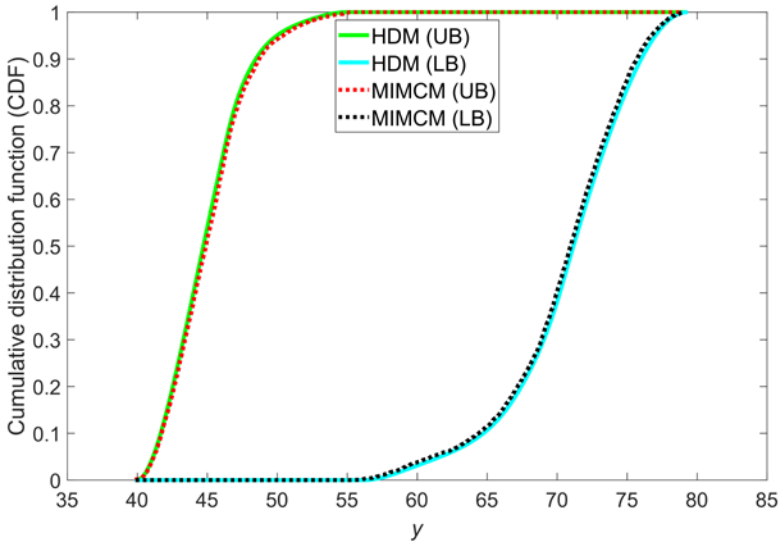

Fig. 4 The UB and LB of the CDF of *y* obtained by HDM and MIMCM

It can be seen from Figure 4 and Table 2 that the upper bound and lower bound of the CDF of *y* calculated by the MIMCM are very close to the referenced results calculated by HDM, which indicates that the proposed MIMCM is feasible and of good accuracy. In this case, the computation process of HDM contains 4×10^6 interval analyses based on original function, even using a less accurate perturbation-based method, it will need to call the original function 4×10^6 times, not to mention the Monte Carlo method. As a contrast, the computational cost of MIMCM includes 84 original function calls for the construction of SGPSM and 5000 interval analyses based on SGPSM. In addition, the computation complexity of the surrogate model is usually much less than that of the original model. Thus, it can be concluded that the MIMCM is more efficient than the HDM but without losing accuracy, especially for the uncertain problems involving multiple p-box variables.

Table 2 The relative errors between the results obtained by HDM and MIMCM

CDF	Lower bound of *y*			Upper bound of *y*		
value	HDM	MMICM	RE	HDM	MMICM	RE
0.1	41.6707	41.7433	0.17%	64.7255	64.3860	0.52%
0.2	42.5339	42.6407	0.25%	67.4361	67.1596	0.41%
0.3	43.2900	43.3929	0.24%	69.0466	68.8656	0.26%
0.4	44.0080	44.1471	0.32%	70.1896	69.9548	0.33%
0.5	45.1451	44.9076	0.53%	71.1558	70.9618	0.27%
0.6	45.4316	45.6516	0.48%	72.1749	71.9393	0.33%
0.7	46.1597	46.3057	0.32%	73.2694	73.0323	0.32%
0.8	46.9995	47.1812	0.39%	74.5043	74.2874	0.29%

0.9	48.4697	48.7104	0.50%	76.0094	75.7069	0.40%

5.2Hexahedral box

Figure 5 depicts a cavity enclosed by a hexahedral box of dimensions 0.25m× 0.25m×0.25m. The acoustic field is surrounded by a clamped plate and five rigid walls, and the center of the top surface is excited by a concentrated harmonic load F=10N. The clamped plate is discretized by 64 four-node Kirchhoff plate elements and the acoustic domain consists of 512 eight-node hexahedral elements.

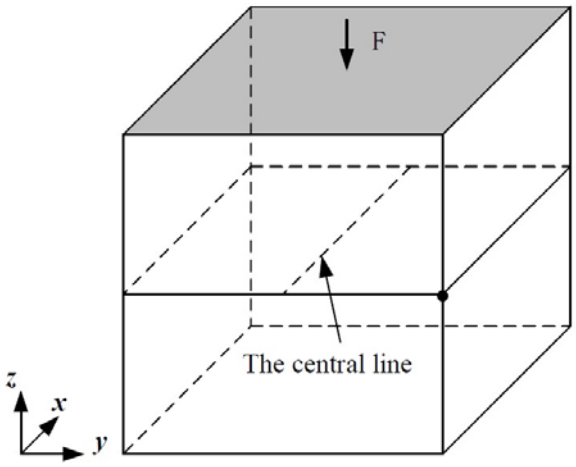

Fig. 5 A hexahedral box

The macro clamped is composed of a periodic uniform material and its equivalent macro material properties can be calculated through the homogenization method [45]. Figure 6 depicts a unit Representative Volume Element (RVE) of the unidirectional fiber reinforced composite. The microstructure unit cell is composed of two prescribed materials, namely, the strong material (Red color) and the soft material (Blue color). The Young's modulus and mass density of the strong material are E_1=210 GPa and ρ_1=7800 kg/m^3, while those of the soft material are E_2=21 GPa and ρ=780kg/m^3,

respectively. The Poisson's ratio for both types of materials is 0.3. Assuming that the unit cells at the micro scale are square of dimensionless length 1×1, and the radius of the fiber at the center of the matrix is 0.2. The finite element model of the RVE consists of 340 elements and 361 nodes.

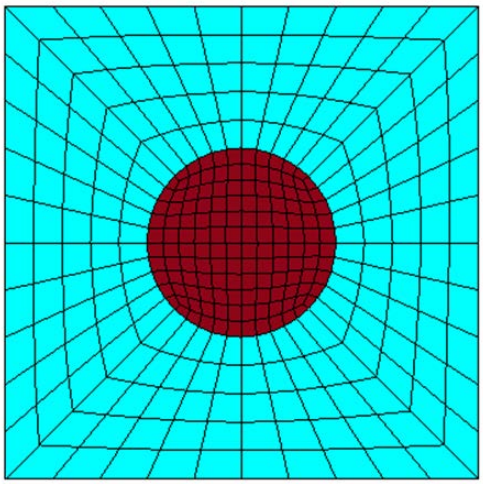

Fig. 6 RVE of a unidirectional fiber reinforced composite

In practical engineering, the uncertainties inevitably exist in the composite structure-acoustic system. Considering the unpredictability of the composite material properties, the type of PDF of composite material property parameter usually is known but the distributed parameter maybe an interval due to the lack of information. Hence the Young's modulus and the mass density of the fiber and the matrix are assumed as p-box variables, whose variation ranges are assumed as E_1=[168, 252] GPa, ρ_1=[6240, 9360] kg/m^3, E_2=[16.8, 25.2] GPa and ρ_2=[624, 936] kg/m^3, respectively. The detail probabilistic information of these variables is listed in Table 3. Considering the impact of external environment change, the sound speed of the air c which is susceptible to temperature is assumed as an interval variable. The variation range of c is assumed as

c= [269.52, 404.28] m/s. Considering manufacturing and assembly errors, the uncertainty of the plate thickness *t* can be reduced by expert opinions based on evidence theory, therefore *t* is assumed as evidence variable. The focal elements and BPAs of *t* are listed in Table 4.

Table 3 The distribution type and probabilistic information of variables.

Variable	Distribution	Probabilistic information	
E_1 (GPa)	Uniform	Parameter $a \in [168, 222.6]$	Parameter $b \in [197.4, 252]$
E_2 (GPa)	Uniform	Parameter $a \in [16.8, 21.84]$	Parameter $b \in [20.16, 25.2]$
ρ_1 (kg/m^3)	Gaussian	Mean $\mu \in [6600, 9000]$	Standard deviation σ =120
ρ_2 (kg/m^3)	Gaussian	Mean $\mu \in [660, 900]$	Standard deviation σ =12

Table 4 The BPAs of evidence variable *t*.

Focal elements (mm)	BPA
[0.9, 0.925]	0.05
[0.925, 0.95]	0.15
[0.95, 0.975]	0.15
[0.975, 1]	0.3
[1, 1.025]	0.1
[1.025, 1.05]	0.1
[1.05, 1.075]	0.05
[1.075, 1.1]	0.1

It should be pointed out that HDM will not be used as reference in this case due to the excessive computation burden for billions inteval finite element calculations. Instead, in order to compare the efficiency with the proposed MIMCM, the traditional Gegenbauer polynomial surrogate model (TGPSM) is applied for the interval analysis in IMCM and this method is called IMCM-TGPSM. The bounds of CDF of the sound pressure amplitude at the point x=0 mm when frequency=50Hz is calculated. In order to guarantee the accuracy, the retained order related to each varible in TGPSM is 3, which means the sampling points is $N_{\text{tot}}=(3+1)^6=4096$. Here, this surrogate model is defined as a higher-order TGPSM (HTGPSM) and the result obtained by IMCM-

HTGPSM is shown as solid line in Figure 10. When the precision requirement is satisfied, the retained order related to each varible in SGPSM is 3, namely the sampling points is N_C=84. The result calculated by MIMCM is shown as broken line in Figure 10. As a contrast, let the retained order related to each variable in TGPSM is set as [1,1,1,1,1,1,2], then the interpolation points is N_{tot}= 96, which is a little bigger than that of SGPSM. Here, this model is defined as lower-order TGPSM (LTGPSM) and the result obtained by IMCM-LTGPSM is shown as dotted line in Figure 7.

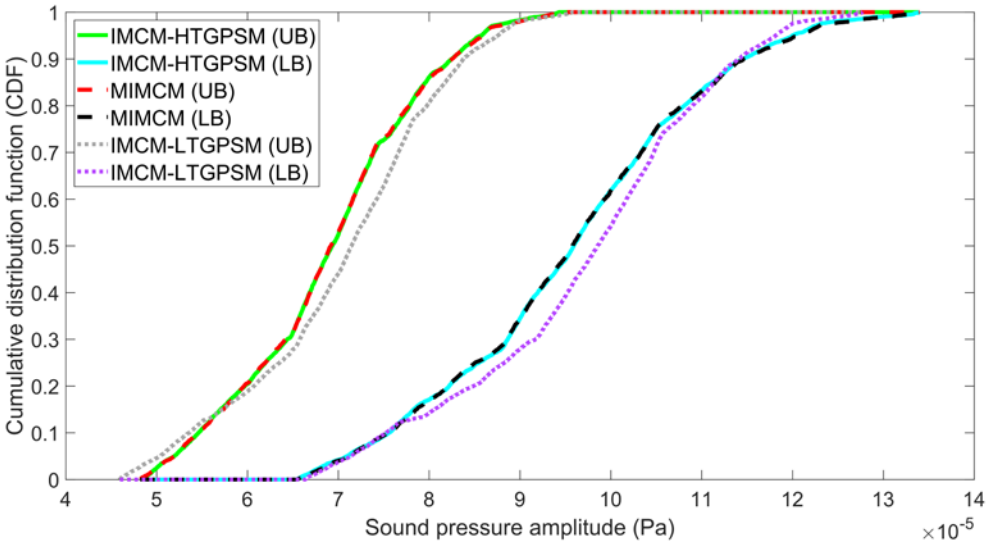

Fig. 7 Bounds of CDF of sound pressure amplitude obatined by different methods at the point x=0 mm when frequency=50Hz.

It can be found from Figure 7 that the bounds of CDF of sound pressure amplitude calculated by MIMCM and IMCM-HTGPSM match well, but the sampling points of SGPSM in MIMCM is far less than HTGPSM. Besides, the bounds of CDF of sound pressure amplitude calculted by IMCM-LTGPSM is out of kilter compared with the IMCM-HTGPSM and MIMCM. This means that the accuracy of MIMCM is better than the IMCM-TGPSM when the sampling points in TGPSM and SGPSM are close. It can

be concluded that the MIMCM is more efficient than the IMCM-TGPSM but with maintaining good accuracy.

Considering the excitation frequency is 50Hz, here the proposed MIMCM is applied to predict the variation range of sound pressure amplitude. Figure 8 shows the variation range of sound pressure amplitude (risk and conservative estimation) of each node at the central line at the 90% confidence level. Here, the variation range of sound pressure amplitude at 90% confidence level refers to the variation range of sound pressure amplitude corresponding to 5% and 95% CDF value. It can be seen from Figure that the UB and LB of risk estimation are both smaller than the UB and LB of conservative estimation. This phenomenon is justified because that conservative estimation usually requires more consideration of possible scenarios than risk estimation in reliability analysis. Therefore, the bounds obtained by conservative estimation is larger than the bounds obtained by risk estimation, which makes the bounds of conservative estimation include the case that the bounds of risk estimation are not considered.

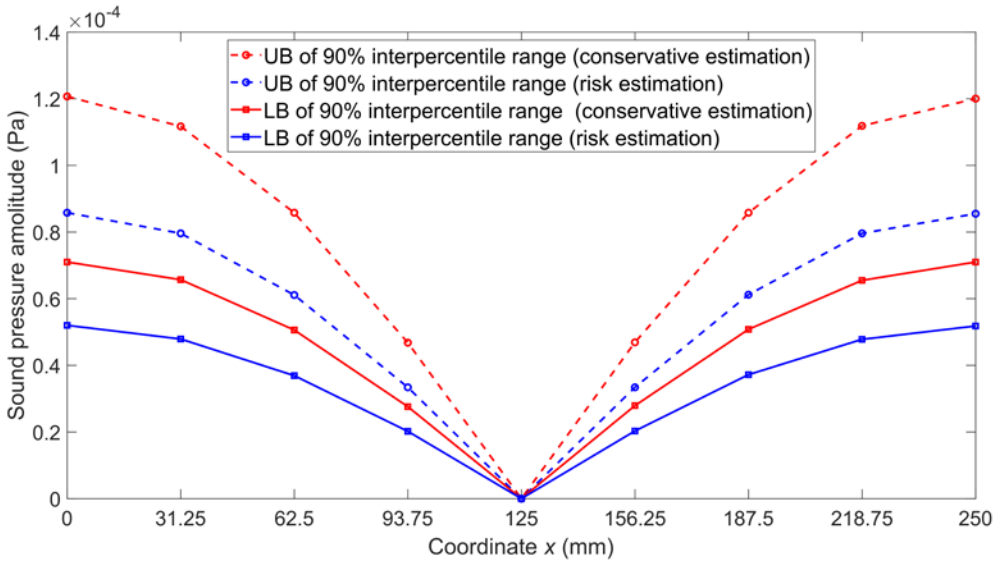

Fig. 8 Range of sound pressure amplitude variation of each node at the central line at the 90% confidence level

5.3Automobile passenger compartment

An automobile passenger compartment with flexible roof panel is shown in Figure 9. The roof panel is excited by a unit normal harmonic point force at the center, whose four sides are fixed. Assuming that the roof panel is composed of periodic composite materials, and the unit RVE of the periodic composite material is the same as that in Section 5.2. The position of node A is close to that of the driver's left ear.

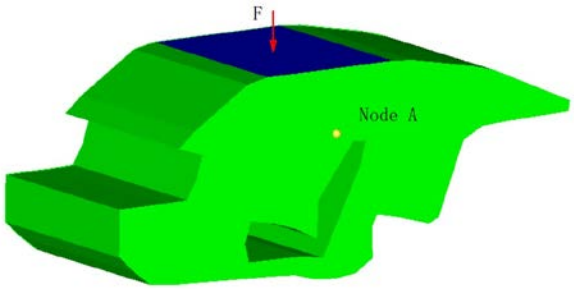

Fig. 9 An automobile passenger compartment

Considering the uncertainty in microscopic material properties of the composite material, the Young’s modulus and the mass density of the fiber and the matrix are

assumed as p-box variables, whose variation ranges are assumed as E_1=[189, 221] GPa, ρ_1=[7020, 8580] kg/m^3, E_2=[18.9, 22.1] GPa and ρ_2=[702, 858] kg/m^3, respectively. Considering the unpredictability of environment temperature, the sound speed of the air is assumed as interval variable, whose variation range is assumed as c= [303.21, 370.59] m/s. Consider manufacturing and assembly errors, the thickness of the plate t is assumed as evidence variable, whose focal elements and BPAs are listed in Table 4. The detail distribution type and probabilistic information of other variables are listed in Table 5.

Table 5 The distribution and probabilistic information of variables

Variable	Distribution	Probabilistic information	
E_1 (GPa)	Uniform	Mean $\mu \in$ [202.5, 207.5]	Standard deviation σ = 4.5
E_2 (GPa)	Uniform	Mean $\mu \in$ [20.4, 20.6]	Standard deviation σ = 0.5
ρ_1 (kg/m^3)	Gaussian	Parameter $a \in$ [7020, 7917]	Parameter $b \in$ [7683, 8580]
ρ_2 (kg/m^3)	Gaussian	Parameter $a \in$ [702, 799.5]	Parameter $b \in$ [760.5, 858]

In this case, the bounds of CDF of the sound pressure amplitude at the Node A when frequency=50Hz is calculated. In order to guarantee the accuracy, the ratained order related to each variable in TGPSM is set as 3, namely $N_{\text{tot}}=(3+1)^6=4096$ times finite element calculations are needed to constuct TGPSM. As a contrast, the ratained order related to each variable in SGPSM is 3. Namely the number of finite element calculations for constructing SGPSM is N_{C}=84, which is much less than that for the TGPSM. Besides, here the first-order matrix decompositon perturbation method (FMDPM) is also introduced for interval analysis in the IMCM and this method is defined as IMCM-FMDPM. Figure 10 shows that the UB and LB of CDF of the sound

pressure amplitude obtained through IMCM-TGPSM and MIMCM are nearly the same, which furthur indicates the efficiency advantage of the MIMCM. Note that the bounds of CDF of the response calculated by IMCM-FMDPM is wider than those obtained by MIMCM and IMCM-TGPSM. The reason of this phenomenon is the truncation of the higher order terms of the Taylor series expansion in the first-order perturbation method. When the FMDPM is employed to interval analysis in IMCM, the times of finite element matrix assembly are greatly reduced, but the total times of matrix calculation is still remaining the same, which means its computational burden is still large. Moreover, the proposed MIMCM can achive a better accuracy, this means it has a good prospect of engineering application.

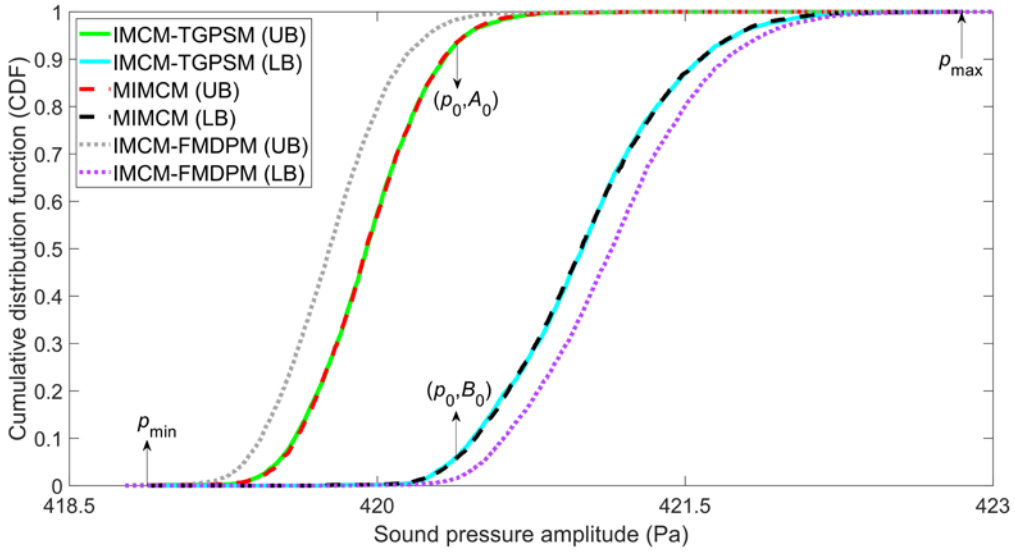

Fig. 10 Bounds of sound pressure amplitude obtained by different methods at the Node A when frequency=50Hz.

In engineering practice, it is necessary to optimize the design of the structure in order to obtain a high level of NVH performance. Generally, the limit amplitude of a target frequency will be set in this process. Then the response amplitude after

optimization design needs to be lower than this limit amplitude. Take the sound pressure amplitude response of Node A as an example. Assuming that its limit sound pressure amplitude is p_0 at the frequency 50Hz. If $p_0 < p_{min}$, it means that the acoustic design of the composite structural-acoustic system model is invalid. If $p > p_{max}$, it means that the acoustic design meets the design requirements. Note that when $p_{min} < p_0 < p_{max}$ as shown in Figure 10, the left boundary value A_0 of the probability cumulative distribution function corresponding to the x-coordinate p_0 is larger than the right boundary value B_0 of the probability cumulative distribution function. This is because that A_0 is a risk estimate, which is the sum of all or part of the probability distributions that contain events of $p \leqslant p_0$; whereas B_0 is a conservative estimate, which is the sum of all the probability distributions that contain events of $p \leqslant p_0$. Thus, risk and conservative reliability analysis based on acoustic performance can be conducted by comparing the design requirements with the response of the composite structural-acoustic system.

Figure 11 depicts the variation range of sound pressure amplitude at Node A under 90% confidence level considering the frequency from 50Hz to 350Hz. Figure 11 shows that the interval of 90% interpercentile range for both conservative estimation and risk estimation expand as the frequency increases, which means the composite structural-acoustic system is more affected by input uncertainties as the frequency increases. Since the MIMCM can quantify the propagation of hybrid and epistemic uncertainties efficiently and accurately, it can play an important role in acoustic design and optimization of practical engineering.

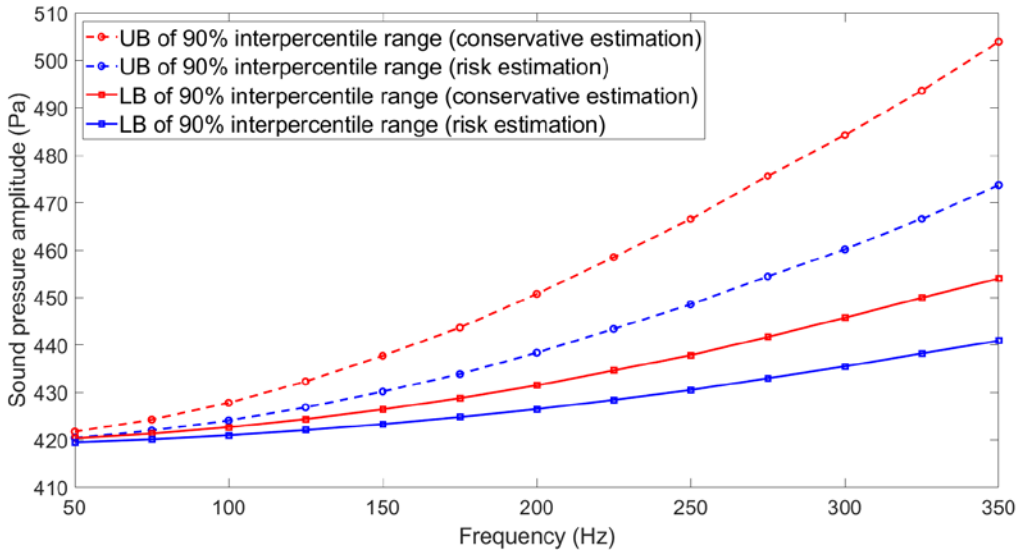

Fig. 11 Variation range of sound pressure amplitude at the Node A under 90% confidence level considering the frequency from 50Hz to 350Hz.

6 Conclusions

In this paper, a probability-box-based method, termed as modified interval Monte Carlo method, is developed for propagation of multiple types of epistemic uncertainties in the response analysis of the composite structural-acoustic system. The multiple types of epistemic uncertainties refer to p-box variables, evidence variables and interval variables, which can all be represented by an equivalent p-box form through a transformation process. To reduce the computational cost of repetitive interval calculations, the sparse Gegenbauer polynomial surrogate model of the composite structural-acoustic system is constructed to increase the efficiency. A numerical example of a nonlinear function is analyzed to verify the accuracy and efficiency of the proposed method. Then two engineering examples of composite structural-acoustic systems involving multiple types of epistemic uncertainties are discussed to further illustrate the efficiency of the proposed method. Numerical results indicate that the

proposed method can achieve both accuracy and efficiency. Moreover, by using the proposed method, risk and conservative reliability analysis based on acoustic performance are conducted by comparing the design requirements with the response of the composite structural-acoustic system.

Therefore, in practical acoustic design and optimization, the proposed method is a considerable method for quantifying the effects of multiple types of epistemic uncertainties on the response analysis of composite structural-acoustic systems. Besides, the proposed method also has good application potential in analysis of other engineering systems involving multiple types of epistemic uncertainties.

Acknowledgement

The paper is supported by the Foundation for Innovative Research Groups of the National Natural Science Foundation of China (Grant No. 51621004), the National Natural Science Foundation of China (Grant No. 51905162), the Natural Science Foundation of Hunan Province (Grant No. 2019JJ50062) and the Fundamental Research Funds for the Central Universities (Grant No. 531107051148). The authors would also like to thank reviewers for their valuable suggestions.

List of acronyms

MIMCM	modified interval Monte Carlo method
IMCM	interval Monte Carlo method
SGPSM	sparse Gegenbauer polynomial surrogate model
HDM	hybrid discrete method
UB/LB	upper bound/lower bound
TGPSM	traditional Gegenbauer polynomial surrogate model
HTGPSM	higher-order traditional Gegenbauer polynomial surrogate model
LTGPSM	lower-order traditional Gegenbauer polynomial surrogate model
FMDPM	first-order matrix decompositon perturbation method

Appendix. Gegenbauer series expansion method

Gegenbauer polynomials $G_n(\xi)$ of n degree can be defined as

$$\begin{cases} G_0^{\lambda}(\xi) = 1 \\ G_1^{\lambda}(\xi) = 2\lambda\xi \\ (n+1)G_{n+1}^{\lambda}(\xi) = 2(n+\lambda)\xi G_n^{\lambda}(\xi) - (n+2\lambda-1)G_{n-1}^{\lambda}(\xi), n \geq 2 \end{cases} \tag{50}$$

In which λ is a polynomial parameter and $\lambda > 0$.

The orthogonality relationship of Gegenbauer polynomials defined on $\xi \in$ [-1, 1] can be represented as

$$\int_{-1}^{1} \rho^{\lambda}(\xi) G_i^{\lambda}(\xi) G_j^{\lambda}(\xi) dx = \begin{cases} h_i^{\lambda}, & i = j \\ 0, & i \neq j \end{cases} \tag{51}$$

In which

$$\begin{aligned} &\rho^{\lambda}(\xi) = k_{\lambda}(1-\xi^2)^{\lambda-(1/2)}, \; k_{\lambda} = \frac{\Gamma(\lambda+1)}{\Gamma(1/2)\Gamma(\lambda+(1/2))} \\ &h_i^{\lambda} = \frac{2^{1-2\lambda}\Gamma(\lambda+1)\pi}{i!(i+\lambda)\Gamma^2(\lambda)} \end{aligned} \tag{52}$$

Where $\rho^{\lambda}(\xi)$ is the weight function. $\Gamma(\bullet)$ denotes the Gamma function.

Based on the orthogonal relationships of Gegenbauer polynomials, a continuous function $f(\xi)$ defined on $\xi \in$ [-1, 1] can be approximated as follows

$$f(\xi) \approx \varphi_N(\xi) = \sum_{i=0}^{N} f_i G_i^{\lambda}(\xi) \tag{53}$$

In which N represents the retained order, f_i is the ith (i = 0, 1,…, N) constant coefficient.

By the use of weighted least squares method and Gauss-Gegenbauer integration formula [46], the coefficient can be obtained by the following equation

$$f_i = \frac{1}{h_i^{\lambda}} \int_{-1}^{1} \rho^{\lambda}(\xi) f(\xi) G_i^{\lambda} d\xi \approx \frac{1}{h_i^{\lambda}} \left(\sum_{j=1}^{m} f(\hat{\xi}_j^{\lambda}) G_i(\hat{\xi}_j^{\lambda}) A_j^{\lambda} \right) \tag{54}$$

In which m is the total number of the interpolation points, the interpolation points $\hat{\xi}_j^{\lambda} (j = 1, 2, ..., m)$ are the roots of $G_m^{\lambda}(\xi)$. A_j^{λ} denotes the weight function and can be represented as

$$A_j^{\lambda} = 2^{2-2\lambda} \pi \left(\Gamma(\lambda) \right)^{-2} \frac{\Gamma(2\lambda + m)}{\Gamma(1+m)} (1 - x_j^2)^{-1} \left(G_m^{\lambda'}(x_j) \right)^{-2}, \quad j = 0, 1, ..., m \tag{55}$$

In which $G_m^{\lambda'}(x_j) = 2\lambda G_{m-1}^{\lambda+1}$.

As for the L-dimensional problems, the function $f(\boldsymbol{\xi})$ can be approximated by the Gegenbauer polynomials and expressed as

$$f(\boldsymbol{\xi}) = \sum_{i_1=0}^{N_1} \cdots \sum_{i_L=0}^{N_L} f_{i_1,...,i_L} G_{i_1,...,i_L}^{\lambda_1,...,\lambda_L}(\boldsymbol{\xi}). \tag{56}$$

where N_l (l=1,2,…,L) is the retained order related to ξ_l, which can be estimated by using the relative improvement criterion [42]. $G_{i_1,...,i_L}^{\lambda_1,...,\lambda_L}(\boldsymbol{\xi}) = G_{i_1}^{\lambda_1}(\xi_1) \cdots G_{i_L}^{\lambda_L}(\xi_L)$. $f_{i_1,...,i_L}$ is the L-dimensional expansion coefficient and can be calculated by

$$\begin{aligned} f_{i_1,...,i_L} &= \frac{1}{h_1^{\lambda_1} \times \cdots \times h_L^{\lambda_L}} \int_{-1}^{1} \cdots \int_{-1}^{1} \rho_{i_1,...,i_L}(\boldsymbol{\xi}) f(\boldsymbol{\xi}) G_{i_1,...,i_L}(\boldsymbol{\xi}) d\xi_1 \cdots d\xi_2 \\ &\approx \frac{1}{h_1^{\lambda_1} \times \cdots \times h_L^{\lambda_L}} \sum_{j_1=1}^{m_1} \cdots \sum_{j_L=1}^{m_L} f(\hat{\xi}_{j_1}, ..., \hat{\xi}_{j_L}) G_{i_1,...,i_L}(\hat{\xi}_{j_1}, ..., \hat{\xi}_{j_L}) A_{j_1,...,j_L} \end{aligned} \tag{57}$$

Where $\hat{\xi}_{j_1}, ..., \hat{\xi}_{j_L}$ represents the interpolation points, $A_{j_1,...,j_L}$ denotes the weight function which can be obtained by

$$A_{j_1,...,j_L} = A_{j_1}^{\lambda_1} \times A_{j_2}^{\lambda_2} \times \cdots \times A_{j_L}^{\lambda_L}. \tag{58}$$

Generally, the number of the interpolation points in relation to ξ_i is set as $m_i = N_i +$

1 in order to strike a good balance between efficiency and accuracy. For the L-dimensional problems, the total number of the interpolation is

$$N_{\text{total}} = (N_1 + 1) \times (N_2 + 1) \times \cdots \times (N_L + 1) \tag{59}$$

References

1. Nefske, D.J., J.A. Wolf, and L.J. Howell, *Structural-acoustic finite element analysis of the automobile passenger compartment: A review of current practice.* Journal of Sound and Vibration, 1982. **80**(2): p. 247-266.
2. Hoffman, F.O. and J.S. Hammonds, *Propagation of uncertainty in risk assessments: the need to distinguish between uncertainty due to lack of knowledge and uncertainty due to variability.* Risk Analysis An Official Publication of the Society for Risk Analysis, 1994. **14**(5): p. 707-712.
3. Hurtado, J.E. and A.H. Barbat, *Monte Carlo techniques in computational stochastic mechanics.* Archives of Computational Methods in Engineering, 1998. **5**(1): p. 3.
4. Spanos, P.D. and A. Kontsos, *A multiscale Monte Carlo finite element method for determining mechanical properties of polymer nanocomposites.* Probabilistic Engineering Mechanics, 2008. **23**(4): p. 456-470.
5. Doltsinis, I. and Z. Kang, *Perturbation-based stochastic FE analysis and robust design of inelastic deformation processes.* Computer Methods in Applied Mechanics & Engineering, 2006. **195**(19): p. 2231-2251.
6. Kamiński, M.M., *A generalized stochastic perturbation technique for plasticity problems.* Computational Mechanics, 2010. **45**(4): p. 349.
7. Lazarov, B.S., M. Schevenels, and O. Sigmund, *Topology optimization with geometric uncertainties by perturbation techniques.* International Journal for Numerical Methods in Engineering, 2012. **90**(11): p. 1321-1336.
8. Ghanem, R.G. and P.D. Spanos, *Stochastic Finite Elements: A Spectral Approach*. 1991: Springer Berlin.
9. Nouy, A., *Recent Developments in Spectral Stochastic Methods for the Numerical Solution of Stochastic Partial Differential Equations.* Archives of Computational Methods in Engineering, 2009. **16**(3): p. 251-285.
10. WU, et al., *A complementary note on Gegenbauer polynomial approximation for random response problem of stochastic structure.* Probabilistic Engineering Mechanics, 2006. **21**(4): p. 410-419.
11. Ben-Haim, Y. and I. Elishakoff, *Convex Models of Uncertainty in Applied Mechanics*. 1990: Elsevier Publishing Company.
12. Oberkampf, W.L., et al., *Challenge problems: uncertainty in system response given uncertain parameters.* Reliability Engineering & System Safety, 2004. **85**(1): p. 11-19.
13. Mcwilliam, S., *Anti-optimisation of uncertain structures using interval analysis.* Computers & Structures, 2001. **79**(4): p. 421-430.
14. Shafer, G., *A Mathematical Theory of Evidence*. 1976: Princeton University Press.
15. Beer, M., S. Ferson, and V. Kreinovich, *Imprecise probabilities in engineering analyses.* Mechanical Systems and Signal Processing, 2013. **37**(1): p. 4-29.
16. Zhang, H., et al., *Structural reliability analysis on the basis of small samples: An interval quasi-Monte Carlo method.* Mechanical Systems and Signal Processing, 2013. **37**(1): p. 137-151.
17. Crespo, L.G., S.P. Kenny, and D.P. Giesy, *Reliability analysis of polynomial systems subject to p-box uncertainties.* Mechanical Systems & Signal Processing, 2013. **37**(1-2): p. 121-136.
18. Liu, H.B., et al., *Uncertainty propagation analysis using sparse grid technique and saddlepoint approximation based on parameterized p-box representation.* Structural & Multidisciplinary

Optimization, 2019: p. 1-14.
19. Wei, P., et al., *Non-intrusive stochastic analysis with parameterized imprecise probability models: I. Performance estimation.* Mechanical Systems and Signal Processing, 2019. **124**: p. 349-368.
20. Wei, P., et al., *Non-intrusive stochastic analysis with parameterized imprecise probability models: II. Reliability and rare events analysis.* Mechanical Systems and Signal Processing, 2019. **126**: p. 227-247.
21. Wu, D. and W. Gao, *Uncertain static plane stress analysis with interval fields.* International Journal for Numerical Methods in Engineering, 2017. **110**(13): p. 1272-1300.
22. Huang, Z.L., et al., *A decoupling approach for evidence-theory-based reliability design optimization*. Structural & Multidisciplinary Optimization, 2017. **56**(1): p. 647-661.
23. Wang, C. and Z. Qiu, *Improved numerical prediction and reliability-based optimization of transient heat conduction problem with interval parameters.* Structural & Multidisciplinary Optimization, 2015. **51**(1): p. 113-123.
24. Xia, B. and D. Yu, *Interval analysis of acoustic field with uncertain-but-bounded parameters.* Computers & Structures, 2012. **112-113**(12): p. 235-244.
25. Lü, H., W.-B. Shangguan, and D. Yu, *A unified method and its application to brake instability analysis involving different types of epistemic uncertainties.* Applied Mathematical Modelling, 2017. **56**: p. 158-171.
26. Xu, M., Z. Qiu, and X. Wang, *Uncertainty propagation in SEA for structural–acoustic coupled systems with non-deterministic parameters.* Journal of Sound & Vibration, 2014. **333**(17): p. 3949-3965.
27. Yin, S., et al., *A new evidence-theory-based method for response analysis of acoustic system with epistemic uncertainty by using Jacobi expansion.* Computer Methods in Applied Mechanics & Engineering, 2017. **322**: p. 419-440.
28. Chen, N., et al., *Uncertainty analysis of a structural–acoustic problem using imprecise probabilities based on p-box representations.* Mechanical Systems and Signal Processing, 2016. **80**: p. 45-57.
29. Wu, D. and W. Gao, *Hybrid uncertain static analysis with random and interval fields.* Computer Methods in Applied Mechanics & Engineering, 2016. **315**: p. 222-246.
30. A. Sofi, E.R., *A unified response surface framework for the interval and stochastic finite element analysis of structures with uncertain parameters.* Probabilistic Engineering Mechanics, 2018: **54**: p:25-36.
31. Wang, M. and Q. Huang, *A new hybrid uncertain analysis method for structural-acoustic systems with random and interval parameters.* Computers & Structures, 2016. **175**: p. 15-28.
32. Chen, N., et al., *A polynomial expansion approach for response analysis of periodical composite structural-acoustic problems with multiscale mixed aleatory and epistemic uncertainties.* Computer Methods in Applied Mechanics and Engineering, 2018. **342**: p. 509-531.
33. Yin, S., et al., *A unified model approach for probability response analysis of structure-acoustic system with random and epistemic uncertainties.* Mechanical Systems & Signal Processing, 2018. **111**: p. 509-528.
34. Schöbi, R. and B.J.J.o.C.P. Sudret, *Uncertainty propagation of p-boxes using sparse polynomial chaos expansions.* Journal of Computational Physics, 2017. **339**: p. 307-327.
35. Ferson, S., et al., *Constructing Probability Boxes and Dempster-Shafer Structures*. 2003: Sandia

National Laboratories.
36. Ferson, S., et al., *Dependence in Dempster-Shafer Theory and Probability Bounds Analysis.* 2004.
37. Ferson, S. and J.G. Hajagos, *Arithmetic with uncertain numbers: rigorous and (often) best possible answers.* Reliability Engineering & System Safety, 2004. **85**(1): p. 135-152.
38. Tonon, F., *Using random set theory to propagate epistemic uncertainty through a mechanical system.* Reliability Engineering & System Safety, 2004. **85**(1-3): p. 169-181.
39. Chen, N., et al., *Hybrid interval and random analysis for structural-acoustic systems including periodical composites and multi-scale bounded hybrid uncertain parameters.* 2019. **115**: p. 524-544.
40. Zhang, H., R.L. Mullen, and R.L. Muhanna, *Interval Monte Carlo methods for structural reliability.* Structural Safety, 2010. **32**(3): p. 183-190.
41. Chao, L., et al., *Sparse regression Chebyshev polynomial interval method for nonlinear dynamic systems under uncertainty.* Applied Mathematical Modelling, 2017.**51**: p. 505-525.
42. Yin, S., et al., *Interval and random analysis for structure–acoustic systems with large uncertain-but-bounded parameters.* Computer Methods in Applied Mechanics and Engineering, 2016. **305**: p. 910-935.
43. Morris, M.D. and T.J. Mitchell, *Exploratory designs for computational experiments ☆.* Journal of Statistical Planning & Inference, 1995. **43**(3): p. 381-402.
44. Chen, J., B. Xia, and L. Jian, *A sparse polynomial surrogate model for phononic crystals with uncertain parameters.* Computer Methods in Applied Mechanics & Engineering, 2018. **339**: p. 681-703.
45. Bendsøe, M.P. and N. Kikuchi, *Generating optimal topologies in structural design using a homogenization method.* Computer Methods in Applied Mechanics & Engineering, 1988. **71**(2): p. 197-224.
46. G. Szegö, *Orthogonal polynomials*. 4th ed. Colloquium Publications. Vol. 23. 1975: American Mathematical Society.